

From Images to 3D models: A photogrammetric approach

Fahad Aljohani⁽¹⁾

1. Introduction

1.1 Background

The foundations of photogrammetry are obviously related to advancements in science and technology. In fact, the four main stages of the development of photogrammetry are directly correlated with the discoveries of photography, aeroplanes, computers and electrical devices. Photogrammetry started at the time that photography was invented by Niepce and Daguerre in the year 1839. From mid-end of the 20th century, photogrammetry was in an innovative and investigational stage with outstanding accomplishments in the terrestrial and balloon fields. The second phase, typically called analogue photogrammetry, is marked by the creation of stereo photogrammetry by Pulfrich (1901). This led to the development of the stereo plotter by Orel, in the year 1908. Aeroplanes in addition to cameras became functional during WWI. The fundamentals of aerial survey techniques were produced between WWI and WWII; these principles are still in use.

Analogue rectification in addition to stereo plotting tools, built on the principles of mechanical and optical technology, were made available around this time. Thus, photogrammetry was recognized as a competent surveying and mapping technique. The fundamental mathematical theory was understood, yet the amount of calculation was unreasonable. As a result, all work was geared toward analogy procedures. Unsurprisingly, Von Gruber referred to photogrammetry as the art of eluding calculations.

Once the computer was made, the third phase started as analytical photogrammetry. Schmid was one of the pioneer photogrammetrists

⁽¹⁾ فهد الجهني: محاضر بقسم جغرافيا ونظم المعلومات الجغرافية – جامعة الملك عبد العزيز.

with a computer. He founded the core of analytical photogrammetry in the 1950s by employing matrix algebra. This was the first time that the adjustment theory was scientifically applied to photogrammetric measurements. Nevertheless, it took many years for computer programs to be made available. Brown created a block adjustment program with bundles in the late 1960s. This was before Ackermann accounted a program that employed independent models as the primary theory. Consequently, the accuracy of aerial triangulation was enhanced by a factor of ten.

The analytical plotter is a second major innovation of the third stage. Once again, there was a delay between the creation and introduction of the tool. It was Helava who created the analytical plotter in the late 1950s. Just the same, the instruments became available to the masses only in the 1970s.

Digital photogrammetry as the fourth stage is swiftly rising as a new area in photogrammetry. Compared to the other stages, digital images are employed in place of aerial photographs. With devices for storage, allowing speedy access to images in the digital format, in addition to chips for micro processing, digital photogrammetry started a few years back. The discipline is new, and not applied by photogrammetric practitioners thus far.

1.2 Related research

The market for 3D maps has been rapidly developing from the time the interactive movie-map was created at the Massachusetts Institute of Technology (MIT) in the late 1970s (Naimark, 1997). A large number of digital map users have started using 3D maps as their primary choice, thanks to advancements in mapping technology. In the future, mapping may describe objective geometry in order to reliably construct high-quality map data, and emphasize community mapping; the maps of the future would incorporate reality sense. The subsequent stage of map services would make information more relevant, giving people what they desire and the background of places that interest them. This stage links geographic location and cultural location. It suggests that maps would not only illustrate the geometric location, but they would also depict the world clearly and change meaningful information into positioning.

Map services make popular use of 2D maps. They generate summaries of street geometry and steer users in 2D spaces. However, users cannot experience true-to-life situations with these maps, taking them to places they desire. As user interests develop, 3D maps can be advantageous both for navigation purposes and interactive operations. Geographic applications apply Virtual Reality, e.g. reproductions of land and urban locations. On 3D maps, the envisioned association between actual and virtual objects augments the navigational value of 3D maps (Hu et al. 2009). These maps do not only allow geospatial data mining, but they also produce a sense of place that the user finds of interest.

Models of 3D maps are typically categorized as two types: model-based maps and image-based maps. Model-based maps make use of huge accumulations of data to create precise 3D models. The execution of positioning in addition to spatial measurement on 3D maps are typically observed as they relate to photogrammetry. In the field of photogrammetry, positioning, geo-referencing, and issues of quality are rather advanced. Geo-referencing is the most favourable method to swiftly integrate with acquisition of 3D data. It was discovered in 1980s, and released in the market in early 1990 (Hutton & Mostafa, 2005). Contrasted with conventional geo-referencing, as referenced by Baltsavias (1999) and Cramer et al (2000) in their research, direct geo-referencing is effective. It permits steering 3D coordinate acquisition owing to a combination of the Inertial System (INS) and GPS. This system of combination can track positions and outward orientation data of sensors, leading to elimination of the need for ground control whilst calculating 3D positions of things. Cramer (2001) examined the effectiveness of the system with direct geo-referencing to augment the performance of photogrammetry.

How to position and control quality in photogrammetry have been continually researched. The first theory was formulated in the mid-nineteenth century (Jiang et al, 2006). By and large, it has been applied to connect world coordinate frames with image coordinate frames. Centimetre levels can be arrived at with accuracy. Collinear Equations, Space Resection, Space Intersection and Direct Linear Transformation are examples of classic algorithms. Maas (1997)

detailed the logical standard of real-time photogrammetric system with three components. Gruen (2001) has also described these concepts: (1) they flexibly recreate 3-D objects; (2) they are highly accurate and reliable; and (3) they manage quality with measurements of coordinates and results.

On a similar note, computer vision technology can enhance the illustration of 3D maps and the performance of the processes of photogrammetry. The methods of image matching as well as image stitching are employed in the production of 3D maps. Image matching is usually categorized into 2 types: i) gray-based matching; and ii) feature-based matching. states that gray-based matching relies on the application of a point-centred template patch in the pictures whilst contrasting the pixel correlation with another representation along with a line that is epipolar. The point which has the highest correlation is believed to correspond with the original point. Scale-invariant feature transform (SIFT) is popularly used for matching features, which are slightly distorted from the image scale and revolution when lit up, and while the image noise is taken into consideration. Candidate matching components can be discovered using the Euclidean distances of their feature vectors.

1.3 Research aims

Photogrammetry is a method to determine the location, shape, and size of object in given pictures rather than by direct measurement. Close-range photogrammetry refers to the method used when the size of an object is less than 100 meters, and the camera is close to the object. Pictures are made from the camera positioned all around the object of interest. The camera axes are parallel in only certain shots. They are generally convergent.

Photogrammetry typically defines the location of a point by a 3D Cartesian co-ordinate system. The original location, the scale and the direction of the object may be randomly defined. It is usually a requisite to shift between co-ordinates in systems with different original locations, directions and scales. This project aims to construct a 3D model by employing Photomodeler 6.0, comparing the preciseness of the outcome both with and without a calibrated camera.

2. Literature Review

2.1 Concepts of measurable realistic image-based 3D maps

Coordinate systems

Coordinate systems are employed to show the relationship between object and image spaces. There are a couple of primary coordinate systems typically used in photogrammetric mapping: the camera coordinate system and the object coordinate system. The two reference frames for these systems are Cartesian and right-handed (Mikhail et al, 2001). The camera coordinate system is founded on the image coordinate system. It is dissimilar from the image coordinate system.

In the image coordinate system, a picture is a representative of the sensor matrix. There are two dimensions in this matrix, defined in terms of (x, y) . The situation of a point on a picture is represented with a matrix index. This requires systematic allocation to the x-axis from the top to the bottom, and to the y-axis from the left-hand side to the right-hand side. The location of the picture coordinate frame is usually the top right-hand corner of a picture. The scale of the index rises downward in the row. The index rises to the right-hand side of the column, and is expressed with integer values. The frame of camera coordinates determines the original location, referred to as the principal point, and places it around the centre of the picture. It is the original location where the camera's optical axis passes through the centre of perspective and crosses the plane of the picture (Mikhail et al, 2001). The system of camera coordinates is a 3D frame of Cartesian coordinates. Hence, apart from the (x, y) plane, another axis, the z axis, must be introduced. The z axis is perpendicular to the plane of the picture. Thus, the optical axis overlaps the z axis. The z axis is typically negative in value, and defines the principal distance in the practice of photogrammetry.

2.2 Approaches to achieve Object control by Photogrammetry

Available Techniques

The Registration Step normally entails accumulating all data sets in a single coordinate system. One of the registration processes is the multiple point clouds which has 3D coordinate data sets with different axes orientations as well as different origins. In this registration process, manual, semi-automatic and automatic methods are first developed before being evaluated. It is worth to note that 3D transformation is the most suited method of registering such data set types while, on the other hand, photogrammetric solution is best suited for registration of 2D images which have point clouds. What the photo geometry registration process does is to combine the captured photos with 3D coordinates in a single coordinate system. To determine digital images reference points as well as those for scanned points, surveying points which are derived by total station measurement can be used. According to El-Hakim, et al. (2004), this technique can be error prone because it can be operated manually, hence, being largely dependent on human interpretation. Beraldin, et al. (2001), note that: an interactive selection of images and 3D corresponding points leads to the determination of interior and exterior orientations images which are with respect to the point cloud coordinate system. It is important to note that interior orientations should be calculated from a separate laboratory calibration process for one to get reliable information. The results that are achieved should then be put in the bundle adjustment solution. The point marking process, if the right algorithm is used during the placing of artificial targets which entails the use of white circles with black background, can be accurate and automatic. However, it is known that more flexibility can be achieved if natural targets are employed. In addition, natural targets can be employed to determine recent captured photos from pre-scanned objects. An approach that can be used to calculate the digital image exterior orientation parameters with respect to range image coordinate system is the feature based resection (Alshwabke, 2005). The definition of the straight lines in a case of a digital image is required. As noted by Klinec and Fritsch (2003), feature based resection approach uses the modified version of co-linearity equations in determining spatial resection by employing straight lines as tie-information. To solve non-

linear equations, a least squares method can be employed. Ordinarily, therefore, initial values are needed.

Georeferencing Images

Techniques for image georeferencing methods are typically classified into two types: indirect georeferencing and direct georeferencing. The indirect technique considers outward parameters of images as unknowns, and works on them in bundle adjustment. It is the only method of establishing the outward parameters if sensor positions and orientations are not given. Outward parameters for images are approximated from ground control points and their matching image points. This establishes photogrammetric bundle adjustment as a very effective method for determining object points, while interior parameter values might be flawed. Systematic effects left unchanged are completely moved into approximated orientation parameters. Nonetheless, the precision of outward parameters is not as vital, seeing that the precision of object points is most significant (Cramer et al. 2000). Bundle triangulation and DLT are commonly used as indirect techniques of georeferencing imaging.

Direct georeferencing is the procedure employed to generate outward orientation parameters based on position, velocity and attitude on-the-fly. In this case, block adjustment methods during post-processing are not applied (El-Sheimy, 2005). The procedure can be set up when combined GPS/inertial systems are accessible. Whole outward parameters can be determined by these sensors. This technique renders the real camera position and orientation rather important. What is more, the balance of mounted sensors is considered, as this balance can be related to tremendous errors (Cramer et al. 2000). A direct method of georeferencing images is referred to as space intersection.

Collinearity Equation

The linear relationship between two explanatory variables illustrates the connection linking item position, matching picture position and the narrative, meaning they rest in identical line (Luhmann, 2006).

Illustrates the collinearity mathematical expression in his manuscript. The match up of p illustration in the picture organizes the functioning of a camera as Equation 1 shows:

$$p = \begin{bmatrix} x - x_0 \\ y - y_0 \\ -f \end{bmatrix} \quad (1)$$

as x, y represent the picture harmony for the object, while x_0, y_0, f represent the internal factors in a camera.

The matching illustration P within the object harmony structure:

$$P = \begin{bmatrix} X - X_c \\ Y - Y_c \\ Z - Z_c \end{bmatrix} \quad (2)$$

The X_c, Y_c, Z_c represents the match ups of the viewpoint hub of the photo recorder while X, Y and Z stands for the match ups of P illustration in the object harmony border.

Herein this orientation, the camera is classified with a view of nine considerations; moreover the factors are usually partitioned into three internal strictures as well as six external strictures. The internal strictures revere to the basis match ups on x axes and y axis of the picture, still narrate to the inner coordination of a camera, whereas the external strictures signify the spatial spot and course of the picture synchronize method relating to the object match classification. The direction strictures articulated in ω, ϕ and κ concerning the harmonize axis X, Y, Z and subsequently the revolving atmospheres joining all three angles jointly can illustrate the direction correlation between picture coordinate structure and object match up structure:

$$M = \begin{bmatrix} a_{11} & a_{12} & a_{13} \\ a_{21} & a_{22} & a_{23} \\ a_{31} & a_{32} & a_{33} \end{bmatrix} \quad (3)$$

here M stands for orthogonal 3×3 mould, allow the constituents of M survive $a_{11} a_{12} \dots \dots a_{33}$, subsequently these essentials shall be:

$$a_{12} = \cos \omega \sin k + \sin \omega \sin \varphi \cos k$$

$$a_{13} = \sin \omega \sin k - \cos \omega \sin \varphi \cos k$$

$$a_{21} = -\cos \varphi \sin k$$

$$a_{22} = \cos \varphi \cos k - \sin k \sin \varphi \sin k$$

$$a_{23} = \sin \omega \cos k + \cos k \sin \varphi \sin k$$

$$a_{31} = \sin \varphi$$

$$a_{32} = -\sin \omega \cos \varphi$$

In reference to equation (1) as well as equation (2), the connection linking those coordinate structures may be explained as:

$$\begin{bmatrix} x - x_0 \\ y - y_0 \\ -f \end{bmatrix} = k M \begin{bmatrix} X - X_c \\ Y - Y_c \\ Z - Z_c \end{bmatrix} \quad (4)$$

as k is range coordinate, then collinearity coordinates may be obtained from equation (4) as:

$$x - x_0 + \Delta x = -f \frac{a_{11}(X-X_c) + a_{12}(Y-Y_c) + a_{13}(Z-Z_c)}{a_{31}(X-X_c) + a_{32}(Y-Y_c) + a_{33}(Z-Z_c)}$$

$$y - y_0 + \Delta y = -f \frac{a_{21}(X-X_c) + a_{22}(Y-Y_c) + a_{23}(Z-Z_c)}{a_{31}(X-X_c) + a_{32}(Y-Y_c) + a_{33}(Z-Z_c)}$$

(5 and 6)

are the as (x, y) are picture factors of object, (x_0, y_0) are dislocation factors among the definite source of the picture match up and the factual source described by main position, and $(\Delta x, \Delta y)$ adjustments of lens deformation.

Least-Squares Estimation

To establish the exterior parameters, space resection dictates for the availability of control points. In the presence of extra control points, better results are obtained by performing a least-squares solution. The use of a least square solution also serves to allow for the editing of point measurements (Mikhail, 2001). An illustration of the functional and stochastic models of least-squares estimation (LSQ) is shown below; in which $\hat{\alpha}$ relates to $(X, Y, Z, \omega, \phi, \kappa)$:

$$v = A\hat{\alpha} - 1 \quad (7)$$

$$D = \alpha_0^2 Q = \alpha_0^2 P^{-1} \quad (8)$$

$$\hat{\alpha} = \sqrt{\frac{v^T P v}{n-u}} \quad (9)$$

In the case of u unknowns and n observations and in which n is always greater than u , the solution is determined by applying the minimum condition to equation (7), according to Kraus (2004):

$$v^T v = \min; (A\hat{\alpha} - 1)^T (A\hat{\alpha} - 1) = \hat{\alpha}^T A^T A \hat{\alpha} - 2I^T A \hat{\alpha} + I^T I \quad (10)$$

In this case, the solution is (Kraus, 2004):

$$\frac{\partial(v^T v)}{\partial \hat{X}} = 2\hat{X}^T A^T A - 2A^T A = 0$$

$$\hat{X} = (A^T A)^{-1} A^T I \quad (11)$$

$A^T A$ is the matrix of normal equation and A represents the design matrix in least-squares estimation. According to Kraus (2004), the non-linear equation is as shown below:

$$I_1 = f(X_1, X_2, \dots, X_u) \quad (12)$$

Taylor series is usually used for translating non-linear equation into linear equation. In particular, Taylor series expansion serves to iteratively to establish approximations to the unknowns. The equation is expanded according to Kraus (2004) as shown below:

$$I_1 = f(X_1^0, X_2^0, \dots, X_u^0) + \left(\frac{\partial f}{\partial x_1}\right) dX_1 + \left(\frac{\partial f}{\partial x_2}\right) dX_2 + \dots + \left(\frac{\partial f}{\partial x_u}\right) dX_u \quad (13)$$

Where $x_1^0 \dots x_u^0$ are the initial values of u . The expression $\frac{\partial f}{\partial x_k}$ is used for determining the coefficients of the equation and is the value for correcting the current value of u as shown below (Kraus, 2004):

$$I_i = I_i^- - f(X_1^0, X_2^0, \dots, X_u^0) = I_i^- - I_1^0 \quad (14)$$

In this case, \bar{I}_i is taken as the actual value of observations, and I_1^0 is the approximated value of observations. Moreover, in the presence of observations with different levels of accuracy, the weighted observation is determined in the process by incorporating standard deviation as shown below (Kraus, 2004):

$$P_{11} = \begin{pmatrix} \frac{1}{\alpha_1^2} & \dots & \\ & & \frac{1}{\alpha_n^2} \end{pmatrix} \quad (15)$$

This forms the minimum condition for the equation as follows:

$$\hat{X} = (A^T P_{II} A)^{-1} A^T P_{II} I \quad (16)$$

Equation 9 is used for determining the estimated variance of observation by using V and the weight matrix P_{II} . In addition, equation 8 can be used to determine the standard deviations for the individual unknowns; where Q is the weight coefficient.

$$Q_{xx} = (A^T P_{II} A)^{-1} \quad (17)$$

Space resection

Room resection is to gain the external strictures by employing collinearity equations which establish the place plus the approach of camera position in object room. The useful changeable usually comprise of the angle centre, the theory expanse, picture focus. The result is typically the point room camera match ups or/and the direction of camera position. The designed picture station might not be near to the real station owing to projective return, this is the biased return for methodical mistakes by modification in the direction strictures (Mikhail, 2001).

If the internal strictures are identified, the room resection usually needs no less than three non-collinear direction position with reverence to collinear math evaluation. There exist six unidentified limits which need to be settle on, these references the conditions of three station match ups plus the 3 angle like strictures. Every control position is able to generate two picture surveillance equations by way of picture strictures (x, y) . Therefore, three coordinates positions supply six picture surveillance equations which establish 6 unidentified. Nevertheless, the internal strictures are unidentified sometimes. The unidentified differ from six to nine, and 2 additional orientation positions, giving four extra picture surveillance equations, are necessary for the resolution (Luhmann, 2006). If the picture deformation counterbalances (Δ_x, Δ_y) are launched in the math

expressions, the unidentified are eleven in this state of affairs, whereas six preferably dispersed control positions are necessary at minimum. Those unidentified external strictures are originally assessed as the estimated principles in a number of circumstances which were set up to the picture surveillance equations. One sensible technique stand out that the estimated principles are openly calculated with excellent apparatus, like the point evaluated by sum position. Another technique is diminutive picture turning round (Luhmann, 2006). If the control axis of the picture method just about matching to the point control arrangement, the factors X_0, Y_0 , may be resolved starting at the centroid of the coordinate positions, as the $(Z - Z_0)$ may be obtained from the acknowledged picture size along with the standard space.

Bundle Triangulation

Package triangulation would be comprehended as the widespread appearance of distance resection by insertion of extra unidentified for additional pictures and object positions. This is a method for the simultaneous arithmetical ability of an limitless figures of spatially spread pictures; also its surveillance equation for minimum squares change is founded on collinearity also. However the linearised study equation obtain incomplete imitative s not merely for unidentified external strictures for pictures but too for point matches of unidentified position (Luhmann, 2006).

Linearised collinearity equation for package triangulation (Luhmann, 2006):

$$\left\{ \begin{array}{l} x = (x) + \frac{\partial x}{\partial X_s} dX_s + \frac{\partial x}{\partial Y_s} dY_s + \frac{\partial x}{\partial Z_s} dZ_s + \frac{\partial x}{\partial \varphi} d\varphi + \frac{\partial x}{\partial \omega} d\omega + \frac{\partial x}{\partial \kappa} d\kappa \\ \quad - \frac{\partial x}{\partial X_s} dX - \frac{\partial x}{\partial Y_s} dY - \frac{\partial x}{\partial Z_s} dZ \\ y = (y) + \frac{\partial y}{\partial X_s} dX_s + \frac{\partial y}{\partial Y_s} dY_s + \frac{\partial y}{\partial Z_s} dZ_s + \frac{\partial y}{\partial \varphi} d\varphi + \frac{\partial y}{\partial \omega} d\omega + \frac{\partial y}{\partial \kappa} d\kappa \\ \quad - \frac{\partial y}{\partial X_s} dX - \frac{\partial y}{\partial Y_s} dY - \frac{\partial y}{\partial Z_s} dZ \end{array} \right. \quad (18)$$

For merely 2 partly covered pictures, there is no difference among package triangulation and grouping of distance resection and junction as external strictures will be premeditated initially and subsequently object match up for unidentified positions will be diminished by junction or a corresponding method.

Direct Linear Transformation

According to Feng (2002), DLT was established in 1971. This technique is also one of the methods that are based on co-linearity equation. However, it is different with other methods because its observation equation is formed in a different way. The method determines its observation equation by directly relating object coordinates of a point and image coordinates. In addition, this method does not require the estimation of exterior parameters. DLT has two parts: the determination of coefficient1 and the object coordinates of the undetermined points. As noted by Feng (2002), the calculation of coefficient1 can be done as shown in the equation below:

$$\left\{ \begin{array}{l} Xl_1 + Yl_2 + Zl_3 + l_4 + 0 + 0 + 0 + 0 + xXl_9 + xYl_{10} + xZl_{11} + x = 0 \\ 0 + 0 + 0 + 0 + Xl_5 + Yl_6 + Zl_7 + l_8 + yXl_9 + yYl_{10} + yZl_{11} + y = 0 \end{array} \right. \quad (19)$$

The observation equation above shows that image coordinates and object coordinates are combined as a coefficient while L1 through L11 are all exterior and interior images combinations which are treated as unknown parameters. Since the equation above is linear, linearization is not needed. Therefore, the estimation of both the interior and exterior parameters is avoided.

2.3 Image processing for computable realistic image – based 3D maps.

Introduction

Processing of images is focused on the features of image matching as well as stitching, especially for the method of indirect geo-referencing. Feature-based and gray-based matching are included in image matching. This is popularly applied in healthcare, remote sensing, in addition to industrial applications. Regardless of the procedure of image matching, the matching components are the objective that image matching procedures are meant to determine and tie in with similar object features, that is, points, patterns, and edges, in at least two object images (Luhmann et al, 2006).

Feature-based matching determines the components over the pictures, and as many as it can identify, so that more constraints can be supplemented to the models to restrict the space for searching to reduce the process time. All components such as point, line and shape are employed as operators to tally a number of related images. Point matching happens to be the most commonly used technique given that points represent the most fundamental geometry to define the object in an image. Point coordinates are used to identify the outward parameters of a picture. Matching of line and shape are also advantageous to image matching, e.g. for clinical purposes. Scale-invariant Feature Transform (SIFT) matching is a classical feature-based matching technique, where the components are unrelated to image scaling, rotation and illumination changes in part.

Candidate matching components may be discovered using the Euclidean distances of feature vectors (Lowe, 2004). Gray-based matching, also referred to as area-based matching, employs original pixel values to determine the features that correspond in different images. Template and least square matching are commonly applied methods. Gray-based matching entails that geometric constraints such as epipolar lines can enhance the precision and reliability of matching (Luhmann et al, 2006). The straightforward definition of template matching is that a point-centred template patch in pictures contrasts pixel correlations with other pictures along with a line that is epipolar.

The point which has the highest correlation is regarded as corresponding with the point that is original. Template matching necessitates some novel features on pictures – the shapes of window patches can be adaptable so as to effectively determine the match.

In computer vision, image stitching and image mosaicking within photogrammetry are methods of panoramic imagery. A panorama is important for human perspective and usually generates a matter-of-fact feeling for a user of 3D maps. By clicking on or taking the cursor over locations in a panorama, corresponding views are updated. Panoramas employed in this way liberate the user from the conventional linear modes of relating to virtual real-world scenes (Teodosio and Mills, 1993). Firstly, an image is stitched to process an image set, captured with the track of the camera. Models of motion are then related. Next, processed images are aligned as is necessitated by the view that images must not be placed on the same plane. Lastly, combining all features of images into a panoramic image is executed. The flawless boundary between intersecting pictures in relation to the concentration of intersection area is developed. A panorama is subsequently generated with precision.

Image Matching

Feature-based Matching

An image or picture is rendered distinguishable by the exclusiveness of the characteristics or properties possessed by it. These characteristics can be a point, line, or shape that comprise it. The paper predominantly discusses the point matching approach, also known as the feature matching method, over the following sections.

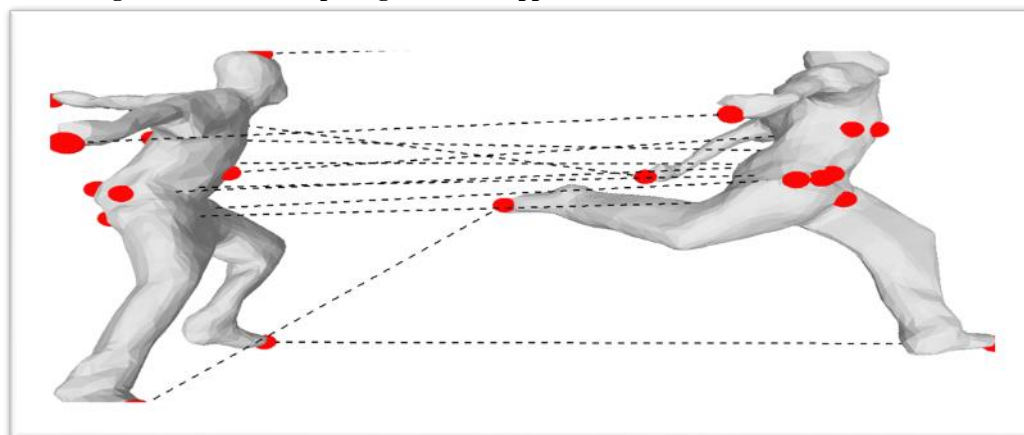


Figure 1. Illustration of point matching

Using the feature matching approach, similar or equal attributes are initially identified in an image. These attributes include curves, edges, angular joints, etc. Post this identification, a thorough assessment is conducted for the collected data. The image gradient plays a critical role in the point feature discovery. The image gradient denotes the degree of change in the pixels. It is vector quantity whose orientation indicates the direction of the speedily moving pixels. The value of the vector denotes the magnitude of the pixel.

The image gradient for each pixel $g(i,j)$ is established by evaluating the difference between the preceding and succeeding pixel. This difference is then used to calculate the magnitude as well as the orientation of the gradient. Numerous operators including the Moravec operator, Forstner operator, local invariance, etc. can be employed for gradient determination. This study discusses the use of the Moravec operator; discussion on other operators exists in Luhmann et al (2006). A Moravec operator with an operational gradient can be found in Luhmann et al (2006).

$$V_1 = \frac{1}{p(q-1)} \sum_{i=-k}^{+k} \sum_{j=-1}^{+1} [g(i,j) - g(i,j+1)]^2 \quad (20)$$

$$V_2 = \frac{1}{(p-1)q} \sum_{i=-k}^{+k-1} \sum_{j=-1}^{+1} [g(i,j) - g(i+1,j)]^2 \quad (21)$$

$$V_3 = \frac{1}{(p-1)(q-1)} \sum_{i=-k}^{+k-1} \sum_{j=-1}^{+1-1} [g(i,j) - g(i+1,j+1)]^2 \quad (22)$$

$$V_4 = \frac{1}{(p-1)(q-1)} \sum_{i=-k}^{+k-1} \sum_{j=-1}^{+1-1} [g(i,j+1) - g(i+1,j)]^2 \quad (23)$$

$$V = \min(V_1, V_2, V_3, V_4) \quad (24)$$

In the above equations, elements V_1, V_2, \dots symbolize the mean square gradient sums evaluated using the window's four primary directions. A feature on the image is distinguished when the value of V , corresponding to the four preliminary direction gradients, exceeds a limit. Elements p and q are connoted by a window of $p \times q$ size respectively. This can be expounded to:

$$p = 2k + 1, \quad q = 2l + 1 \quad (25)$$

Another feature that has been researched extensively is the line characteristic. The line feature is also believed to be a fundamental geometry for feature matching and image detection. The Hough transform method is a highly recognized approach for line detection. Hough transform propounds the use of the Hough parameter space for denoting a line instead of using image space. A review of the Hough transform is depicted in this study. Detailed discussion can be referred in "Fitting: The Hough transform" (2009). The line function in image space is given as follows (Goshtasby, 2005):

$$y = mx + b \quad (26)$$

Here, x and y represent the co-ordinates of the image, whereas m and b indicate the slope and the y -intercept of the line respectively. This suggests that every image co-ordinate pair (x,y) relates to a

unique point (m,b) in the Hough parameter space. The value of factor b can be ascertained by the following equation:

$$b = -mx - y \quad (27)$$

A limitation exists, though, in the Hough space. This limitation is related to the orientation of the line. If the line is aligned in a perpendicular direction to the axes in the Hough space, it entails the existence of infinite Hough parameters like b or m by the vertical lines. The Hough transform is optionally given using the polar coordinate system. The function for the same is expressed as below (Goshtasby, 2005):

$$\rho = (x - x_c) \cos \theta + (y - y_c) \sin \theta \quad (28)$$

Here, ρ denotes the image center and the line distance, x_c, y_c are the image center coordinates, (x, y) are the point coordinates and the parameter θ here is the angle from the x axis to the line. It has limitations in conjunction with the rows and columns of the image. The θ ranges within 360 degrees.

Yet another convention of matching is scale space of the image. This approach dwells on the notion of image pyramids. Processing of a sequence of diverse samples at different levels of an image is carried out in pyramids.

Every sample is averaged against a 2:1 sub sample image at the succeeding level. Contemporary approach of the scale space attempts to describe that the pyramid level is not suggested by the sub-sampling of the image, instead it is distorted with the same image. Also, the size of the distorted image is the same as the original image. In order to instigate the obscureness of the original image having a variance of σ^2 , the Gaussian process is used. σ is known as the scale parameter. σ vacillates at differing levels. A high level of the scale indicates a higher σ .

SIFT Matching

In 2004, David G. Lowe, a computer expert in computer science department of University of British Columbia in Canada released the SIFT, a matching algorithm for distinctive features. The SIFT employs detectors to determine ideal image points with a representative orientation and scale, and also a SIFT descriptors that expresses the optimal points in which the descriptors are robust to the noise, affine transformation and lighting, hence allows image correspondences to be matched accurately.

The detection of SIFT keypoint entails two stages of scale-space extrema and a keypoint localization.

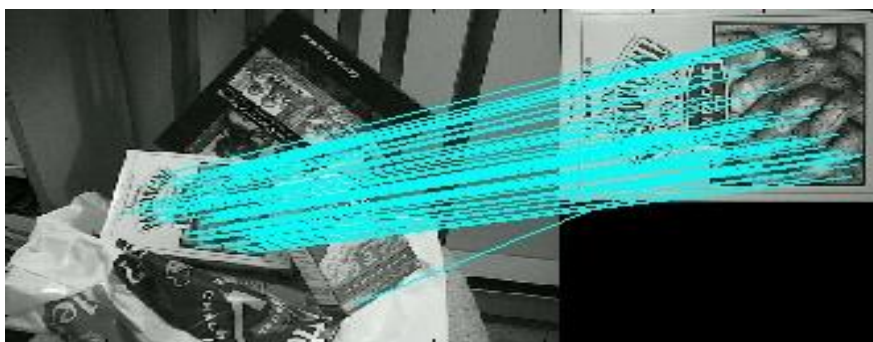


Figure 2. SIFT matching

The scale- space extrema helps in locating the potential interest points of all scales and image locations (Lowe, 2004). The Difference-of-Gaussian (DOG) is an algorithm that has been demonstrated by Koenderink (1984) and Lindeberg (1994) to be efficient in detection of SIFT keypoint. The DOG functions, as defined by Lowe (2004) can be demonstrated as below;

$$L(x, y, \sigma) = G(x, y, \sigma) * I(X, Y) \quad (29)$$

Where $L(x, y, \sigma)$ is the function of scale space of an image, and the operator $*$ represents convolution computation, while $I(X, Y)$ refer to the input image and $G(x, y, \sigma)$ is the function of variable scale Gaussian that is expressed further in Lowe (2004) as below;

$$G(x, y, \sigma) = \frac{1}{2\pi\sigma^2} e^{-(x^2+y^2)/2\sigma^2} \quad (30)$$

The process of scale-space extrema relies on the constant K that is obtained in computing the difference in two neighboring scales. The function $D(x, y, \sigma)$ of the scale-space extrema defined in Lowe (2004) can be represented as below;

$$D(x, y, \sigma) = (G(x, y, k_\sigma) - G(x, y, \sigma)) * I(x, y) = L(x, y, k_\sigma) - L(x, y, \sigma) \quad (31)$$

The extrema according to Lowe (2004) is efficient according to DOG procedure since two images involved in deduct, which maxima and minima of DOG images are obtained by comparing neighboring pixels to each other. Localization of the keypoint is then employed to narrow down the searched accurate point in the pixel which is then referenced to the scale of other pixels around the same point. Filtering of bad points is essential once the candidate point of extrema which is close to true extrema is obtained in the sample. Use of Taylor-expansion on the scale-space function $D(x, y, \sigma)$ is necessary in eliminating the problem of bad points. The function according to Lowe (2004) is represented as below;

$$D(X) = D + \frac{\delta D^T}{\delta X} X + \frac{1}{2} X^T \frac{\delta^2 D}{\delta X^2} X, \quad X = (x, y, \sigma)^T \quad (32)$$

Where D is based on the sample point, and x is the compensation between the sample point and the true extrema point. The derivative function of X^T can be obtained when there is a set to zero, as illustrated by Lowe (2004) as;

$$\hat{x} = - \frac{\delta^2 D^{-1} \delta D}{dX^2 \delta X}$$

(33)

According to Lowe, the derivative of D is a rough estimate of a difference of two sample points. The \hat{x} can be conceded onto its sample point that evaluates the interpolated location of its extremum. The extremum location of value D (\hat{x}) can then be obtained by substituting equation 33 and 32 as shown by Lowe (2004);

$$D(\hat{x}) = D + \frac{1}{2} \frac{\delta D^T}{\delta X} \hat{x}$$

(34)

The set of good points I obtained via the method of DOG and scale-space extrema, and on the other hand generated SIFT descriptors employs gradient orientation and magnitude in eliminating the rotation and scale effects by assigning all the properties of local image to the keypoint descriptor. The scale-invariant feature is implemented by use of scale keypoint that is compared to the smoothed Gaussian scale image, and thus treated to be similar if images are very close. Pixel differences are used to generate the gradient orientation $\theta(x, y)$ and the magnitude $m(x, y)$ of each image, as illustrated by Lowe (2004) as;

$$\theta(x, y) = \tan^{-1} ((L(x, y + 1) - L(x, y - 1)) / (L(x, y + 1) - L(x, y - 1)))$$

(35)

$$M(x, y) = \sqrt{(L(x + 1, y) - L(x - 1, y))^2 + (L(x, y + 1) - L(x, y - 1))^2}$$

(36)

A gradient histogram with 36 groups of a gradient orientation on a scale of 360 degrees is created in which each bin of the histogram with a range of 10 degrees describes the dominant gradient direction. The highest bar of the histogram represents the dominant direction of the local gradient; while the weight of the sample pixels passed into the histograms is evaluated by using gradient magnitude and Gaussian-weighted circular window which is 1.5 times the scale of SIFT keypoint (Lowe, 2004). As indicated in the paper Ke and Sukthankar (2004), the corresponding distances and ratio test points in the SIFT descriptors is merged, and on the other hand, (Fischler & Bolles 1981) notes that, an adjustment of a Random Sample Consensus (RANSAC) algorithm is essential during SIFT processing operations.

Gray-based matching

Gray-based matching is a procedure of matching the templates, which centres on the geometrical, correlation, and radio-metrical transmutation of elements a picture (pixel) with the adjacent pixels. In employing this technique, an individual ought to apply the same algorithmic rule that has been formerly utilized in matching. For instance, while matching the templates in a couplet of images, it is requisite that a designate point be carefully chosen on the image of reference utilized. Then from the designate point that was chosen, a pertinent template is at this juncture spawned. This procedure continues with the subsequent procedure involving creation of different template, through applying transmutations that project the angles of the archetype template onto a different image in duos, on the adjoining image.

Correlation of the elements of picture is applied in order to define a templates correspondence. Initially, a minimum correlation limit is established for evaluating correlation of pixels in the correspondence analysis. Then, when the highest correlation match is achieved amid the image of reference and the partnering image, the resultant point has been accurately predicted. Especially during the time when the geometric limitation is been incorporated in the model for matching.

The highly utilized algorithmic rules in gray-based matching are estimation of the least square and correlation.

According to Lutemann et al (2006) the correlation technique employed to come up with an estimate of similarity, through measuring engrafts in the pixels and then matching the template patch's unique patterns to the referential image and the pulled out patch to the image targeted. The fundamentality of similarity processes with regard to standard deviations and covariance is the dynamic of cross-correlation coefficient.

$$\rho_{fg} = \frac{\sigma_{fg}}{\sigma_f \sigma_g} \quad (37)$$

Where σ_{fg} , σ_f , σ_g the correlation function elements with fg with respect to f (x, y) and g (x, y) can be expanded as (Luhmann et al, 2006):

$$\sigma_{fg} = \frac{\sum[(f_i - \bar{f})(g_i - \bar{g})]}{n} \quad (38)$$

$$\sigma_f = \sqrt{\frac{\sum(f_i - \bar{f})^2}{n}} \quad (39)$$

$$\sigma_g = \sqrt{\frac{\sum(g_i - \bar{g})^2}{n}} \quad (40)$$

Where (\bar{f}, \bar{g}) and "n" are the arithmetic average of the pixel value and pixels enumerate of in template patch, correspondingly. Cross-correlation coefficient is calculated in every locus of targeted image, and the precise location of the patch is calculated with that if the coefficient in terms of x and y positions on the targeted image, which normally is greater than a verge. Then, the commensurateness of the carefully chosen point in the referential image is keyed out. The threshold fundamentally is contingent on the content of the image. The problematic area in regards to the correlation technique is that, the variance in scales amid the referential image and the image of target brings about differences of correspondence measures. This identical

result was established by revolving or even warping the images (Luhmann et al, 2006).

Estimation of the least square as applied in gray-based matching has been analysed for a considerable period of time. The precept of this methodology is established in that reduction of the value differences of pixel amid the referential image and the image of target images via the restraint re-counts to geometry. The geometric limitation is subjugated to the copulate template patches that protrude into a level object area. The perception midpoints of the pictures as well have to be charted by means of using perception protrusion (Luhmann et al, 2006):

$$f(x, y) - e(x, y) = g(x, y) \quad (41)$$

The elements $f(x,y)$ and $g(x,y)$ indicate the dual image templates, whereas $e(x, y)$ is the sound element. Every single distinct pixel measure on the image of reference has the analogous geometrically transmuted pixel measure on the image of target. The accruing equation of observation is linearized as (Luhmann et al, 2006):

$$f(x, y) - e(x, y) = g^o(x, y) + g_x da_o + g_x x da_1 + g_x y da_2 + g_y db_0 + g_y x db_1 + g_y y db_2 + r_0 + r_1 g^o(x, y) \quad (42)$$

where g_x, g_y , partial derivative discrepancies in regards to the gradient pixel value, are as follows (Luhmann et al, 2006):

$$g_x = \frac{\partial g^o(x,y)}{\partial x}, g_y = \frac{\partial g^o(x,y)}{\partial y} \quad (43)$$

Once estimation least squares technique is applied in this equation, the least squares operational and stochastic representations are (Luhmann et al, 2006):

$$I_{n.1} + V_{n.1} = A_{n.u} \hat{x}_{n.1} \quad (44)$$

In which “n” denotes pixels number in the template, while “u” denotes the enumerate of unknowns

$$\hat{x}_{n,1}^T = [da_0, da_1, da_2, db_1, db_2, r_0, r_1] \quad (45)$$

$$\hat{x} = (A^T P A)^{-1} (A^T P I) \quad (46)$$

$$\hat{x} = \sqrt{\frac{v^T P v}{n-u}} \quad (47)$$

The weightiness of “P” is generally appraised with “I”. The reiteration of least squares procedure is probable up until all the unknowns attained as well as correctly valued.

Both the least squares and correlation procedures propose to quest the commensurateness starting from the initial pixel to the last pixel, except when the commensurateness is keyed out. It might call for an extended period of time for the duration of the procedures. The geometric restraints for instance lines and epipolar planes were brought in to address the subject of deficiency in proficiency in corresponding.

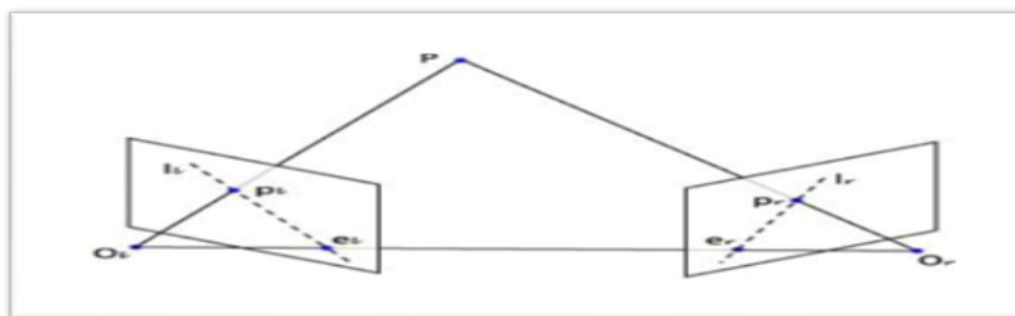


Figure 3. Illustration of Epipolar geometry

The epipolar restrictions is presenting that the point object “p” is juttred out onto the dualistic overlain images, and the points of reference in the images are O_r and O_l correspondingly.

The component “O” denotes to the outlook midpoint of camera. The p , o_r , and o_l as demarcated by the epipolar plane, whereas the epipolar lines were positioned where the epipolar plane intersects with two images, such as the demonstration of l_r and l_l . The epipolar

line may be decided when the images are positioned comparatively (Mikhail et al, 2001). The designation of matching points centred in epipolar geometry for binary images is expressible as in the following equation (Luhmann et al, 2006):

$$P_a = 1 - e^{-\frac{nf}{F}} \quad (48)$$

where P_a represents the prospect of matching point, n is the enumerate of points in the image, f is the range of epipolar space of search, and F is the area of the image. Nevertheless, through the increasing on the quantity of image point n in addition to the space of search f , the likelihood of incompatibilities is also aggregating (Luhmann et al, 2006). On the occasion whereby over two images are applied in matching the commensurateness, the least square technique of matching is the most dependable methodology to handle the byzantine geometry amongst the images. The matching equation (41) would expand to (Luhmann et al, 2006):

$$f(x, y) = e_i(x, y) = g_i(x, y), \quad i = 1, \dots, m \quad (49)$$

Whereby “ i ” is the single image in the multiple-image collection. At that point, the least square estimate might be comported in derived simulations terms.

Template matching

A template outlines the zone of search for charting the original coordinates with its commensurateness. The search zone might be restricted through applying extra restrictions. In lieu of template matching, the utmost established equation would be the squared error, (Snyder, 2004):

$$SE(x, y) = \sum_{\alpha=1}^N \sum_{\beta=1}^N (f(x - \alpha, y - \beta) - T(\alpha, \beta))^2 \quad (50)$$

Whereby the outline is the dimension of $N \times N$ frame, the image f and the template T assume variance at points (x, y) . The equation would be expanded as (Snyder, 2004):

$$SE(x, y) = \frac{\sum_{\alpha=1}^N \sum_{\beta=1}^N f^2(x - \alpha, y - \beta) - 2 \sum_{\alpha=1}^N \sum_{\beta=1}^N f(x - \alpha, y - \beta) T(\alpha, \beta) + \sum_{\alpha=1}^N \sum_{\beta=1}^N T^2(\alpha, \beta)}{\sum_{\alpha=1}^N \sum_{\beta=1}^N T^2(\alpha, \beta)}$$

(51)

To guarantee the excellence of corresponding, a much sophisticated scientific archetypal has been applied while roughly template matching positioned the commensurateness that requires to express the obscurities.

The quality of matching can be described by a set of parameters = (a_1, a_2, \dots, a_n), which may possibly be the picture element themselves (Snyder, 2004).

Snyder well-defined the equation associated with the template as well as the images as $M(a, f(x))$.

The M function primarily is associated to the established of constraint, which are at that point maximized, whilst the x and y coordinates in the template are conceded to the, the procedure of maximizing represented below (Snyder, 2004):

$$M_{a_j} = \frac{\partial M}{\partial a_j} = 0, \text{ for } j = 1, \dots, n. \quad (52)$$

Image Stitching

Image stitching technology uses at least two images from a single scene. Parts of the image intersect – they may depict separate times, different views or use distinct sensors – to create a whole, flawless, high resolution image (Hua et al., 2009). It is a technique to depict a big street scene or landscape by patching images, one to another.

The image stitching procedure is composed of image registration and image calibration. Brown (1992) accounts image registration as a basic undertaking in image processing. This process is employed to tally at least two images, e.g., taken at separate times, using distinct sensors, or from different perspectives.

From Images to 3D models: A photogrammetric approach

Four commonly used methods are correlation and sequential methods, the Fourier method, point mapping and elastic model-based matching. The correlation method uses cross-correlation to stitch images. The sequential method is like the correlation method, which enhances performance by orders of magnitude. However, none of these methods can handle frequency-in-dependent noise. The Fourier method employs Fourier transformation to find the perfect match based on data in the frequency domain. The point mapping method performs image registration according to feature points on all pictures. The control point is of the essence in this approach. The elastic model-based matching technique is a recent development in image registration. This procedure is based on the assumption that registration transformation is caused by twisting an elastic material to a minimum. It is further supposed that the intensity of twisting and stretching are reliant on the energy state of the elastic material. Interpolation that is piecewise and uses Spline is employed whilst using energy to a minimum.

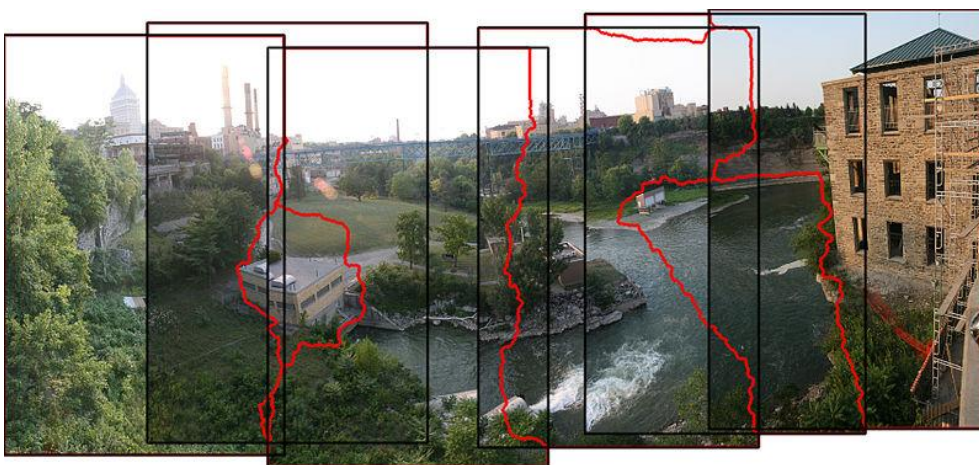


Figure 4.

Example for geometrical registration and stitch line in panorama creation.

The method applying cross-correlation may only be used for minor definite affine transformations as it determines the correspondence of points serially. The Fourier method is restricted for the same reason, yet its efficiency of dealt with frequency-dependent noise is enhanced. Point mapping is employed well for the process with unfamiliar albeit universal transformation. Elastic model-based matching can tackle the most complex transformation by modelling it piece by piece.

Camera Calibration

There are two ways that a camera can be calibrated. First, it can be done in the laboratory. Second, a method called self-calibration which is normally done by using the same project images can also be employed. It is always recommended that self-calibration should be used in a case where images vary in camera settings. In addition, one should consider a number of geometric configurations. For reliable and accurate self-calibration to be determined, those images that restrict imaging must be considered. However, this method is not recommended for some project sites because there is a professional camera which allows one to fix the settings in the field work while at the same time allowing calibration process to be employed. One can use a control field that is shown in the figure below for calibration process.

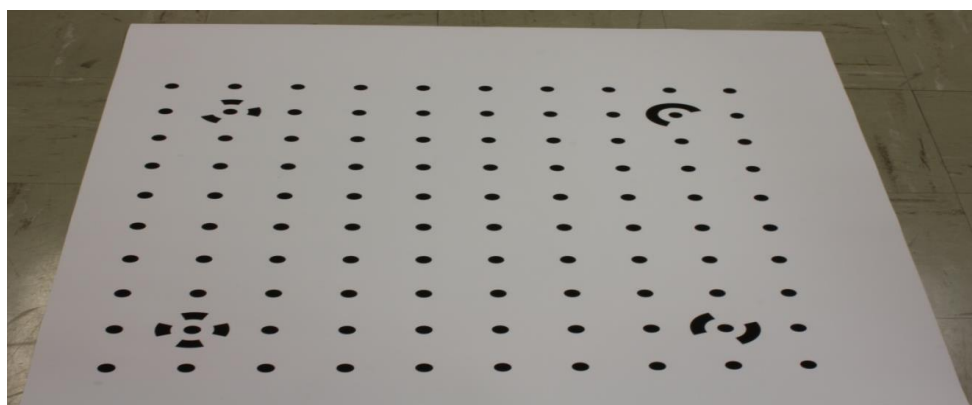


Figure 5. control field for calibration process.

In this field, 110 points with black circles and white a background can be used. The use of this type has a number of advantages. Since the target used is automatic in the sense measuring image coordinates can be attained automatically, human error is avoided. In addition, 12 or more photos can be taken in every control field, both vertically and horizontally, in every calibration process. Using 2D test field helps in getting images at different lengths, hence, one can determine an accurate focal length. To get the principal point, up to three images can be rotated. Canon EOS 450D, a known professional camera with eight mega pixels, can be calibrated to determine a required evaluation test. To achieve this, the lens of the camera can be adjusted indefinitely as well as being fixed. It is also imperative to note that the setting must not be altered during the calibration process. If this is observed, reliable camera parameters can be realized.

3. Experiment and Result Analysis

3.1 Experiment

The word, photogrammetry, suggests that it is a technique to measure objects in an image. A digital photogrammetry system that is integrated is a hardware-software configuration to develop photogrammetric products from digital pictures applying both manual and automated methods. There is high demand for full 3D data for architecture, landscape planning, environmental analysis, tourism etc. To represent the actual situation of an object, and to determine 3D of all edges of the object – especially the inaccessible points of the structure – the development of precise 3D models is a prerequisite. Close-range photogrammetry is a technology to extract 3D points from pictures. These points are helpful for precise 3D modelling, in addition to visualization. Suitable measurements are derived for digital photogrammetry from pictures instead of objects. Thanks to the digital flow of data, photogrammetry is now recognized as an effective alternative to classical building measurement and

reconstruction procedures. In the current project, a scientific experiment has been performed to examine the preciseness of the 3D model produced by the photogrammetric method.

3.2 Experiment Design

This scientific research method was designed to construct a 3D model by employing Photomodeler 6.0. The technology was meant to help compare the preciseness of the outcome both with and without a calibrated camera. The experiment was conducted indoors, using two photographs taken at the School of Civil and Environmental Engineering. Canon 450D was employed for these photos. The calibration file was obtained from Professional Officer Zhou, Y. (2013). Total station was employed to determine the 3D coordinates of GCPs in a system of coordinates that was local. The GCP coordinates were determined by total station.

GCP ID	Ground Truth (m)		
	X	Y	Z
1001	-4.076	6.03	2.075
1002	-3.396	6.015	2.076
1003	-3.395	6.009	0.390
1004	-0.335	5.777	2.081
1005	-0.339	5.745	2.654
1006	0.682	5.748	2.084

Table 1. GCPs Coordinates Information

Also for this experiment, points 1001, 1002, 1003, 1004, 1005, and 1006 were chosen as ground control points to measure the outward parameters of pictures. Images 1 and 2 were used. These images are shown in Figures 5 and 6 respectively.

From Images to 3D models: A photogrammetric approach



Figure 6. Image 1 Indoor Experiment**Figure 7. Image 2 Indoor Experiment**

3.3 Influence and Remarks

Id is defined as the number of point identification that is applied in referencing as it is indicated to the results both with and without a calibrate camera as it is shown in the table below. The presentation of the XYZ values indicate the model coordinates that are calculated during the overall processing, the XYZ values indicates the last column, marking accuracy the pixels RMS residual value attained in the project.

From Images to 3D models: A photogrammetric approach

Point ID	X	Y	Z	X Precision	Y Precision	Z Precision	RMS Residual (pixels)
1008	-2.605	5.993	2.107	0.009	0.023	0.005	0.626
1009	-2.611	5.987	1.671	0.009	0.023	0.004	0.006
1010	-2.405	5.985	2.106	0.008	0.023	0.005	0.928
1011	-2.408	5.968	0.127	0.009	0.026	0.005	1.055
1012	-0.478	5.942	2.119	0.004	0.021	0.005	0.977
1013	-0.464	5.948	0.129	0.005	0.026	0.006	1.593
1014	1.188	5.897	2.075	0.007	0.027	0.006	0.248
1015	0.499	5.938	0.394	0.005	0.026	0.006	1.864
Mean	-1.160	5.957	1.341	0.007	0.024	0.005	0.912

Table2. Accuracy assessment of points with camera calibration

Point ID	X	Y	Z	X Precision	Y Precision	Z Precision	RMS Residual (pixels)
1008	-2.612	5.982	2.107	0.008	0.020	0.004	1.067
1009	-2.620	5.978	1.672	0.007	0.019	0.003	0.082
1010	-2.411	5.972	2.107	0.007	0.019	0.004	1.225
1011	-2.408	5.953	0.128	0.007	0.021	0.004	1.899
1012	-0.473	5.915	2.119	0.003	0.015	0.004	1.275
1013	-0.461	5.931	0.129	0.004	0.018	0.005	1.881
1014	1.181	5.884	2.070	0.005	0.017	0.004	1.247
1015	0.502	5.931	0.395	0.004	0.017	0.005	1.771
Mean	-1.162	5.865	1.340	0.005	0.018	0.004	1.305

Table3. Accuracy assessment of points without camera calibration

According to the outcomes presented in the table above, a comparison made between both with and without a calibrated camera showed that there was a large difference of the X, Y; Z and it was approximately 0.009 m, 0.027 m and 0.005 m respectively. Additionally, there was a larger difference between with and without a calibrated camera of the X, Y, Z precision which was 0.0002m,

0.010m and 0.002m respectively. According to the mean after the calibration of the camera indicated that it was evenly better than without the presence of the calibration of the camera. The main difference of the following axes X,Y,Z was 0.002 m, 0.092 m and 0.001 m respectively, while the difference of the X,Y,Z precision indicated 0.002 m, 0.006 m and 0.001m respectively. RMS being less than the RMS without a calibrated camera improves the results of a calibrated camera.

According to the principles of the photomodeler, in order for a photogrammetric project to be effective the RMS residue value is supposed to be less than 3. Therefore the RMS value for all the points is 1.3 which indicates that it is an effective value for a project.

4. Conclusion

Applications of 3D modelling, both scientific and visual, are on the rise. Products for 3D modelling are employed in many fields. With enhancements in hardware and software, studies in 3D modelling can be conducted more simply and speedily. This project required the construction of a 3D model with the use of Photomodeler 6.0, comparing the preciseness of the outcome both with and without a calibrated camera. Majority of such researches can be conducted by using only images. This is an example of a noncontact technology. What is more, this justifies the use of the photogrammetric method in risky places.

The method may also be considered to survey objects that cannot be directly measured. Thus, the photogrammetric method is safest to use. One of the major attributes of this method is that it requires little time to perform measurements. Administrative work during the phase of evaluation generally takes longer time. Yet another advantage of this method is that it does not ask of the user to possess expert knowledge of photogrammetry. Besides, big investments in equipment are not necessitated. Apart from the classic wireframe models, advancements in close-range photogrammetry permit gathering of new 3D models with textures that are photorealistic. Metric properties are therefore blended with visual information on element materials.

This makes it possible to realize techniques potentialities and significantly enhance outcomes.

5. Reference

1. Alshawabkeh, Y. and Haala, N., 2005. Automatic Multi-Image Photo Texturing of Complex 3D Scenes. CIPA IAPRS Vol. 34-5/C34, pp. 68-73.
2. Angelo, P. (2007), "Radiometric Alignment and Vignetting Calibration", the 5th International Conference on Computer Vision Systems, Bielefeld, Germany, 21-24 March.
3. Baltasvias, E. (1999). "A comparison between photogrammetry and laser scanning." ISPRS Journal of Photogrammetry and Remote Sensing, vol. 54, no. 2-3, pp. 83-94.
4. Bernardini, F., Martin, I., Rushmeier, H., 2001: High-quality texture reconstruction from multiple scans. IEEE Trans. On Visualization & Computer Graphics, Vol. 7(4), pp. 318-332.
5. Brown, L. (1992), "A Survey of Image Registration Techniques", ACM Computing Surveys (CSUR) archive, Vol. 24, No. 4, December, pp. 325 – 376.
6. Brown, M. and Lowe, D.G., 2003. Recognising panoramas. IEEE 9th International Conference on Computer Vision, pp 1218–1225.
7. Cramer, M., Stallmann, D., Haala, N. (2000), "Direct georeferencing using GPS/Inertial exterior orientations for photogrammetric applications", IAPRS, vol XXXIII, Amsterdam, pp. 198-205.
8. Cramer, M., 2001. "Performance of GPS/inertial solutions in photogrammetry.", Photogrammetric Week 01, Wichmann verlag, Heidelberg.
9. El-Hakim, S. F., Beraldin, J.-A. and Blais, F., 2003a. Critical factors and configurations for practical 3D image based modeling. VI Conference on Optical 3D Measurement Techniques, Zurich, Switzerland (Eds. A. Gruen and H. Kahmen). Vol. 2, pp. 159-167.
10. El-Sheimy, N. (2005), "An Overview of Mobile Mapping Systems", Pharaohs to Geoinformatics FIG Working Week

-
- 2005 and GSDI-8, Cairo, April 16-21 Feng, W., "Close Range Photogrammetry", Wuhan University Press, Wuhan, 2002, pp. 142 – 159.
11. Fischler M. A. and Bolles R.C., 1981. Random Sample Consensus: A Paradigm for Model Fitting with Applications to Image Analysis and Automated Cartography. *Communications of the ACM*, vol.24, no.6, pp381–395.
 12. Goldman, D.B., Chen, J.H. (2005), "Vignette and exposure calibration and compensation", In *Proceedings of the 10th International Conference on Computer Vision (ICCV05)*, Washington, USA, pp. 899–906.
 13. Goshtasby, A. A. "2-D and 3-D Image Registration: for Medical, Remote Sensing, and Industrial Applications", John Wiley & Sons, Inc. Publications, 2005.
 14. Grubb, B. (2010), "Conroy: Google Wi-Fi spy was 'deliberate' - Security - News", ZDNet,
 15. Gruen, A and Bar, S 2001, Aerial Mobile Mapping—Georeferencing Without GPS/INS, Institute of Geodesy and Photogrammetry, Zurich.
 16. Hua, Z., Li, Y., Li, J. (2010), "Image stitch algorithm based on SIFT and MVSC", 2010 7th International Conference on Fuzzy Systems and Knowledge Discovery, FSKD 2010, Vol. 6, pp. 2628-2632.
 17. Hu, Q., Liu, S. and Mao, K., 2009. A "Reality Vision" Navigation Technique Based on Sequence Geo Referenced Image Databases, *Critical Issues in Transportation Systems Planning, Development and Management*, ASCE.
 18. Hutton, J. and Mostafa M. M. R., 2005. "10 years of Direct Georeferencing for airborne photogrammetry." *Geo-Information-Systeme*, vol.2005, no. 11, pp. 33-41.
 19. Jiang, Z, Jiang, N, Wang, Y and Zang, B , 2006, Distance measurement in panorama, *Inst. of Elec. and Elec. Eng. Computer Society*, San Antonio, TX, United states.
 20. Ke, Y. and Sukthankar, R. 2004. Pea-sift: A more distinctive representation for local image descriptors. *Computer Vision and Pattern Recognition*, Washington, DC, USA, pages 66-75.

21. Koenderink, J.J., 1984. The structure of images. *Biological Cybernetics*, vol.50, no.5, pp363–37.
22. Klinec, D., and Fritsch, D., 2003, Towards pedestrian navigation and orientation. Proceedings of the 7th South EastAsian Survey Congress: SEASC'03, Hong Kong, November 3-7.
23. Kraus, K, *Photogrammetrie I*, 5th edition, Dümmler Verlag, Bonn, Germany,.
24. Lowe, D. G. 2005, Demo Software: SIFT Keypoint Detector, Luhmann, T. Robson, S. Kyle, S. Harley, I., “Close Range Photogrammetry”, Whittles Publishing, Dunbeath, 2006, pp. 229 – 260.
25. Maas, HG, 1997, "Concepts of real-time photogrammetry." *Human Movement Science*, vol. 16, no. 2-3, pp. 189-199.
26. Mikhail, E.M., Bethel, J.S., and McGlone, J.C. “Introduction to Modern Photogrammetry”. J. Wiley, New York, 2001.
27. Naimark, M. , 1997. A 3D Moviemap and a 3D Panorama. *SPIE Proceedings*, vol.3012, San Jose. Snyder, E.W. and Qi, H. *Machine Vision*. Cambridge University Press, United Kingdom, 2004.
28. Teodosio, L. and Mills, M., 1993. Panoramic overviews for navigating real-world scenes. *Multimedia*.